# Director configuration and self-organization of inclusions in two-dimensional smectic membranes

P. V. Dolganov and V. K. Dolganov
*Institute of Solid State Physics, Russian Academy of Sciences, 142432 Moscow Region, Chernogolovka, Russia*
(Received 3 November 2005; revised manuscript received 24 January 2006; published 18 April 2006)

The behavior of isolated inclusions (nematic droplets, smectic islands) and formation of chains and clusters from inclusions in oriented smectic membranes have been studied. Investigations of inclusions were performed in membranes in which the molecular ordering was oriented by an external magnetic field. At planar boundary conditions on the interface between the membrane and inclusions different configurations of the **c**-director field were observed: Coulombic, dipolar, quadrupolar, and mixed. The observed orientation of inclusions and their interactions and self-organization correlate with the predictions of the theory based on the electromagnetic analogy. Chaining and formation of superstructures differ in oriented and nonoriented membranes.

DOI: 10.1103/PhysRevE.73.041706 PACS number(s): 61.30.Jf, 64.70.Md, 61.30.Gd

## I. INTRODUCTION

The mechanism of interparticle interaction and ordering in systems of large particles are a subject of intensive investigations during recent years [1–6]. Various phenomena in these systems occur in a space-time scale that is real for human perception and such systems are model ones for classical condensed matter physics. Understanding the mechanism of interaction of macroscopic particles is also very essential in many technological applications [7,8]. It has been shown in recent years that macroscopic particles (of micrometer scale and larger) which do not create long-range electric and magnetic fields may effectively interact at distances comparable with and exceeding the sizes of the particles. These interactions may lead to a nontrivial collective behavior of the particles: their structural self-organization and crystallization with formation of "macroscopic" crystals from particles.

In liquid crystals interparticle interactions are related to the distortion of the orientation ordering of the surrounding medium [1,2]. Rigid orientation of molecules on the inclusion boundary leads to elastic deformation of the host medium. Two-dimensional (2D) interaction and inclusion ordering are realized in smectic membranes formed by molecular layers parallel to the free surfaces [9,10]. In the smectic-*C* (Sm*C*) structures considered here, the long axes of molecules (**n** director) are tilted by an angle $\theta$ with respect to the normal of the smectic layer. In-plane molecular orientations form the 2D field of molecular ordering, which is commonly described by a 2D vector, the so-called **c** director [11]. The anisotropic interaction of the inclusions in the plane of the membranes is mediated by elastic deformation of the 2D field of molecular ordering [12]. Theories [12–15] predict possibilities for formation of various structures and orientation of inclusions in 2D systems depending on the anisotropy and strength of the interparticle interaction. Up to now only some of these interactions and structures have been observed experimentally [16–22]. Partially the reason is that investigations were conducted in membranes in which the **c** director was not oriented, which hampered the identification of interactions and investigations of orientational effects. Until the present time the main means of preparation of in-plane oriented membranes is using the electric field in ferroelectric structures. However, this method proved to be poorly applicable for investigations of inclusions. An electric field leads to motion of inclusions (related to conductivity of the membranes) and to partial loss of the **c**-director orientation. Much preferable is usage of a magnetic field, which does not lead to motion of charges and inclusions in membranes. Using a magnetic field we obtained perfectly oriented membranes of large dimensions (up to 1 $cm^2$). Moreover, the magnetic field may be used to study nonpolar Sm*C* membranes, which are not oriented by the electric field. In the present work we performed investigations of inclusions in oriented Sm*C* membranes. We found that formation of chains and clusters from droplets and their orientation differ sufficiently in membranes in which the **c** director was and was not oriented. For a quantitative comparison of theory and experiment measurements on oriented membranes have to be made.

This paper is organized as follows. In Sec. II we describe the details of the experiment. Section III is devoted to studies of molecular configuration around single inclusions. In Sec. IV we describe interparticle interactions leading to formation of linear chains, and in Sec. V we focus on more complex structures. We end by a brief conclusion in Sec. VI.

## II. EXPERIMENT

Membranes were prepared from the smectic liquid crystal undecyl oxybenzoic acid (UDOBA) [23] and its mixtures with decyl oxybenzoic acid (DOBA) [23], both purchased from KhZHR, Kharkov. Bulk samples exhibit the following phase transition temperatures: crystal $\leftrightarrow^{108\ ^\circ C}$ Sm*C* $\leftrightarrow^{122\ ^\circ C}$ nematic $\leftrightarrow^{132\ ^\circ C}$ isotropic (UDOBA) and crystal $\leftrightarrow^{87\ ^\circ C}$ Sm*C* $\leftrightarrow^{122\ ^\circ C}$ nematic $\leftrightarrow^{142\ ^\circ C}$ isotropic (DOBA). Free-standing membranes were prepared by drawing a small amount of the compound in the smectic phase across a circular hole (4 mm diameter) in a thin glass plate. The thickness of the membranes (number of layers *N*) was determined by optical reflectivity measurements. For thick membranes the thickness was determined from the spectral dependence of optical reflectivity in "backward" geometry [24]:

 

$$I(\lambda) = \frac{(n^2-1)^2 \sin^2(2\pi nNd/\lambda)}{4n^2 + (n^2-1)^2 \sin^2(2\pi nNd/\lambda)} \quad (1)$$

where $n$ is the index of refraction, $d$ the layer thickness, and $\lambda$ the wavelength. For thin membranes ($N<15$) the reflected intensity is approximately proportional to $N^2$:

$$I(\lambda) \approx [N\pi d(n^2-1)/\lambda]^2. \quad (2)$$

This allows one to determine the thickness by comparing the reflected intensity from membranes with different numbers of smectic layers. In the Sm$C$ phase the values of optical reflection have been measured for different directions of the plane of polarization of light. Since the index of refraction for light polarization parallel to the **c** director is larger, the light intensity is also larger along this direction. These measurements allow one to determine the direction along which the **c** director is oriented.

In thick membranes nematic droplets nucleate in the vicinity of the bulk smectic-nematic transition temperature. In thinner membranes ($N<20$) the nucleation temperature is shifted to the high-temperature region. Nucleation of a large number of droplets is observed near the temperatures of thinning transitions [25,26]. After nucleation, the size of droplets is very small (less than 5 $\mu$m). The droplet diameter increases with temperature, which is related to increase of the material in the droplet and decrease of the difference between the membrane tension and surface tension of the bulk sample [27]. The typical size of the droplets in our experiments ranged from 8 to 40 $\mu$m. Droplets are preserved in the membrane for a long time. After cooling small droplets disappear; large ones are transformed into smectic islands whose thickness is as a rule much smaller and size much larger than those of the droplets from which the islands formed. The diameter of the islands in our experiments was about 100–150 $\mu$m. Measurements were conducted in magnetic field oblique with respect to the plane of the membrane or in a field parallel to the membrane. The **c** director is oriented along the projection of **H** on the membrane. In oblique fields the **c** director is oriented so that the nematic **n** director makes a smaller angle with **H** [28]. So in our experiments we know the direction of the **c** vector. Droplet nucleation and formation of structures in membranes were observed in an optical microscope equipped with a digital camera. UDOBA and DOBA possess a large in-plane optical anisotropy even near the bulk smectic-nematic transition temperature. This enabled us to visualize in polarized light the in-plane deformation of the **c** director field near isolated droplets and structures formed by droplets.

## III. SINGLE INCLUSIONS IN MEMBRANES

### A. Director field outside the inclusions

The main question which should be answered in investigations of inclusions is the mapping of the director field around individual inclusions. This distribution determines the interaction between the inclusions and types of structures formed by inclusions. Figure 1 shows different types of distortion near the inclusions observed in the membrane. The

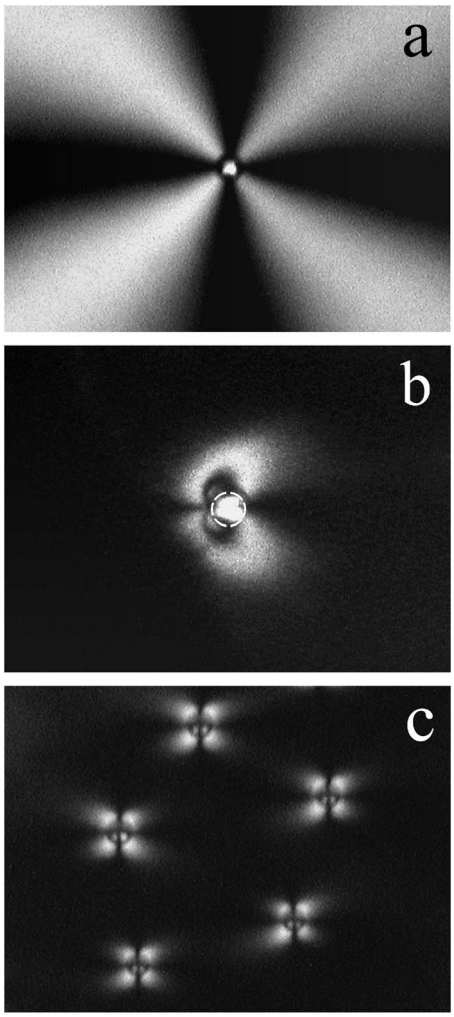


FIG. 1. Nematic droplets nucleated in the smectic membrane with different topology of the **c** director near the droplets: Coulombic (a), dipolar (b), and quadrupolar (c). In (b) and (c) the far-field director is vertical. The magnetic field is applied to the film (b),(c), and vector **c** is oriented from top to bottom. The polarizers are crossed. Bright brushes correspond to oblique **c**-director orientations. For clarity the boundary of the droplet in (b) is marked by a dashed circle. (a) 50% DOBA, 50% UDOBA, $T=125.7$ °C; (b)–(c), UDOBA, $T=126.2$ °C. Each photograph is about 215 $\mu$m wide.

size of the droplets is about 10–11 $\mu$m Figs. 1(a) and 1(c) and about 17 $\mu$m Fig. 1(b). For clarity the boundary of the droplet in Fig. 1(b) is marked by a dashed circle. The images were obtained with polarizer and analyzer crossed. In Figs. 1(b) and 1(c) the orientation of the polarizer was parallel to the orientation of the **c** director far from the inclusions (vertical direction). In such a geometry parts of membranes with director distortion look like bright regions. In the experiments we used weak magnetic fields ($H\sim 10^3$ Oe), which oriented the **c** director at large distances from the droplets, but did not induce essential distortions in the **c** director field near them. The magnetic coherence length in the Sm$C$ structure is $\xi\sim(K/\chi_a)^{1/2}/H\sin\theta$ [28]. For typical values of the elastic constant $K\sim 10^{-6}$ erg, magnetic anisotropy $\chi_a\sim 10^{-7}$, and $\theta\sim 30°$ we shall obtain for $\xi$ a sufficiently large value about 60 $\mu$m. For small droplets (less than 20 $\mu$m in diam-

eter $D$), the main distortion of the **c** director localizes at distances less than 30 $\mu$m from the droplet boundary. This distance (about $1.5D$) is the characteristic length associated with the anchoring. For large smectic islands the distortion of the **c** director induced by the island surface stretches to large distances and is distorted by the magnetic field far from the island. It is worth noting, however, that in nonoriented films (Sec. V) the distortion induced by absence of the **c** director alignment disturbs the inclusion-induced configuration more than the magnetic field. We may state that configuration of the **c** director near inclusions (at distances less than 30 $\mu$m) is governed by the boundary conditions, and magnetic field distortion has little effect on this configuration.

Spatial variation of $\mathbf{c}(\mathbf{R})$ is described by Laplace's equation $\nabla^2\mathbf{c}=0$ [2], the solution of which at large $R$ can be expanded in multipoles: $c_\mu=C^\mu+D^\mu+Q^\mu+\cdots$, where $C^\mu$, $D^\mu$, and $Q^\mu$ describe the Coulombic, dipolar, and quadrupolar parts of the **c** director configuration [2,29]. It is essential that the presence of these terms is dictated by the symmetry of the system [2,29]. For the same global planar orientation of molecules on the inclusion boundary we found three qualitatively different types of director configuration (Fig. 1), the multipolar expansions of which start with $C^\mu$, $D^\mu$, and $Q^\mu$. Rotating the polarizers reveals $C_\infty$ symmetry near the droplet in Fig. 1(a) (Coulombic configuration). The director field near the inclusion is circular. Such an inclusion is equivalent to a defect with topological charge (or winding number) $s=+1$ [11] and it orients the **c** director in the absence of an external field at large distances [Fig. 1(a)]. In a membrane oriented by an external field Coulombic configuration may be observed only near droplets. Far from the droplets four white brushes are grouped into two pairs, forming two $\pi$ walls going away from the droplet. The walls orient parallel to the undistorted **c** director. Such orientation of walls is energetically more favorable. From the symmetry of Figs. 1(b) and 1(c) we can conclude that multipolar expansion starts with the dipolar term for the droplet in Fig. 1(b) ($C_v$ symmetry) and the quadrupolar one for droplets in Fig. 1(c) ($C_{2v}$). The distance at which an essential deformation of the molecular orientation takes place decreases from Coulombic to dipolar and then to quadrupolar configuration. The dipolar configuration [Fig. 1(b)] with orientation of the polar axis perpendicular to the **c** director was predicted by Pettey, Lubensky, and Link [12], however, earlier near droplets it has not been observed. Observations in a magnetic field for different orientations of the polarizer and analyzer enable one to determine the configuration of molecular ordering near the inclusions. Figure 2 shows the director distribution (streamlines of the field) for the three cases observed experimentally. A dipolar configuration with its axis parallel to the far-field **c** director has not been observed in our experiments. The reason is that the equilibrium direction of the dipole is perpendicular to the far-field **c** director for planar boundary conditions [12]. The deviation from this equilibrium configuration leads to increasing distortion of the **c** director and elastic energy [12].

As we mentioned earlier droplets form at heating near or above the temperature of the bulk Sm$C$-nematic transition. Droplets nucleate in different ways in Figs. 1(a)–1(c), which is related to the necessity for conservation of the topological charge of the system. A uniformly oriented sample has zero topological charge; meanwhile a droplet with strong anchoring corresponds to topological charge $s=+1$. So the droplet with director configuration corresponding to $s=+1$ [Fig. 1(a)] cannot nucleate in an oriented membrane since it would change the total topological charge of the system. This droplet [Fig. 1(a)] nucleated upon heating in the center of a point topological defect formed in the process of membrane preparation. Droplets in Figs. 1(b) and 1(c) nucleated in an initially defect-free membrane. Nucleation of these droplets is accompanied by generation of compensating topological defects with total topological charge $-1$ [1–5] to satisfy the topological constraints (charge neutrality in the system). The nature of these defects and their localization (on the droplet boundary or in the host medium) may be different. The symmetry of the droplet with defects is equivalent to the sym-

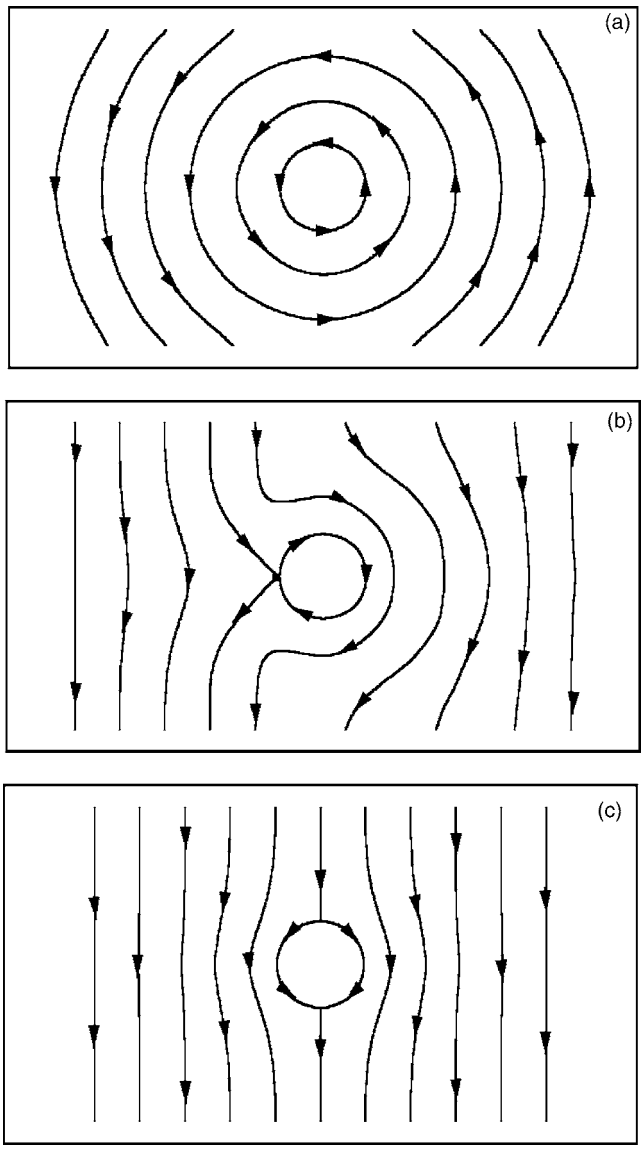


FIG. 2. Schematic representation of the director field around inclusions for three different configurations of elastic deformation: Coulombic (a), dipolar (b), and quadrupolar (c). The arrows show the direction of the **c** vector.

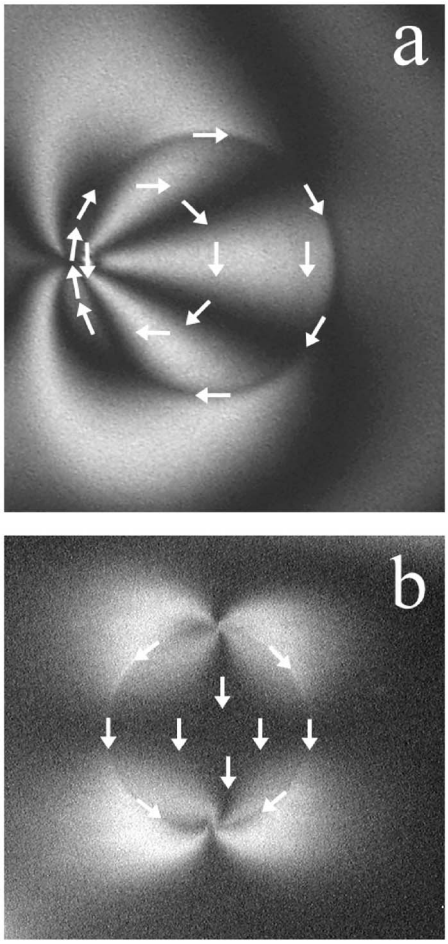


FIG. 3. Smectic islands with dipolar (a) and quadrupolar (b) director field configurations. One (a) or two (b) topological defects are located on the island boundary. The polarizer and the analyzer are crossed. In frame (a) the polarizer is under an angle 36° with respect to the vertical direction. Vector **c** orients from top to bottom far from the inclusions. In (b) the polarizer is vertical (parallel to the **c** director). Arrows show the orientation of the **c** director on the island boundary and inside the island. The frames are about 240 $\mu$m wide. UDOBA, $T=127\,^{\circ}\mathrm{C}$ (a); 50% DOBA, 50% UDOBA, $T=124.5\,^{\circ}\mathrm{C}$ (b).

metry of the director field. In our case one topological defect with $s=-1$ [dipole, Figs. 1(b) and 2(b)] or two defects with $s=-1/2$ [quadrupole, Figs. 1(c) and 2(c)] on the opposite sides of the droplet boundary are formed. The reason for nucleation of droplets with one or two defects up to now is not clear. It may be related to the mechanism of droplet nucleation, the competition between surface and elastic host medium energy, on the microscopic structure of the interface between the droplet and the membrane.

We observed dipolar and quadrupolar director configurations around smectic islands [Figs. 3(a) and 3(b)] with topological defects located at their border. The layer steps impose a tangential alignment on the **c** director [22]. As described above, a way to prepare smectic islands is to cool the membrane with droplets. The tangential alignment of the **c** director and location of topological defects on the interface does not change upon cooling. Inside the islands as well as outside them the **c** director is oriented parallel to their boundary (white arrows in Fig. 3). This orientation forms the characteristic distribution of the **c** director within the inclusions which will be discussed later. As for the interface between the "bulk" nematic droplet and a thin smectic membrane, or the meniscus between the membrane and the bulk reservoir [30], they also may include smectic steps (edge dislocations). The dislocation with its core along the **c** director has a lower energy than the one aligned in the perpendicular direction [31]. This may be the reason for a well-defined planar orientation of the **c** director on the droplet boundary in Sm*C* membranes.

Most theoretical studies [2,4,13–15,32–36] of inclusions in liquid crystal media (except [12] for the dipolar configuration) were made for nematic structures in which the directions **n** and **−n** were equivalent. Let us consider the changes induced by two-dimensionality of the membrane and the vector nature of the **c** director (nonequivalence of **c** and **−c**). In three-dimensional (3D) nematics with planar anchoring the defects must localize on the spherical boundary of the inclusions. This is related to the topology of the sphere, which cannot be filled by the vector field of the **n** director without singularities. The minimal sum of defect indices on a spherical surface is equal to 2, i.e., the Euler character of the surface [37]. The planar 2D geometry increases the number of possible structures: defects may be located both at the border of circular inclusions and near them in host 2D nematic. In a Sm*C* structure the vector nature of the **c** director ($\mathbf{c}\neq-\mathbf{c}$) restricts possible types of defects: two half-integer defects are trapped at the border due to the topological impossibility of the existence of a defect with $s=-1/2$ in the host medium.

The vector nature of the **c** director prohibits a number of 2D configurations, but does not change the appearance of the streamlines near the inclusion when configurations are allowed in both the 2D nematic and Sm*C*. In the one-constant approximation the distribution of the molecular ordering may be written in an analytical form. According to the electromagnetic analogy [12] the director profile, i.e., $(c_x,c_y)=(\cos\varphi,\sin\varphi)$, is the superposition of distributions originating from several topological defects. The distribution of the field of a single charge situated at $R=0$ has the form $\mathrm{Im}\ln(z)$ [12], where $z=x+iy$. Since in our case we know the position of the topological defects (on the inclusion boundary) we should not (contrary to the 2D nematic) conduct the minimization of the free energy to determine the location of defects. For dipolar configuration the solution of Laplace's equation is equivalent to the director field formed by an $s=+2$ defect at the inclusion center and an $s=-2$ defect at $x=R_0$ [Fig. 4(a)]. The distortion amplitude $\varphi(x,y)$ has the form

$$\varphi = 3\pi/2 + 2\,\mathrm{Im}\ln(z) - 2\,\mathrm{Im}\ln(z-R_0). \tag{3}$$

This solution satisfies the planar boundary condition at the inclusion border and becomes uniform at infinity (parallel to the $y$ axis). In the following it will be convenient to consider polar coordinates $(R,\psi)$, where $\psi$ is defined counterclockwise, starting from the direction of the $x$ axis (Fig. 4). The

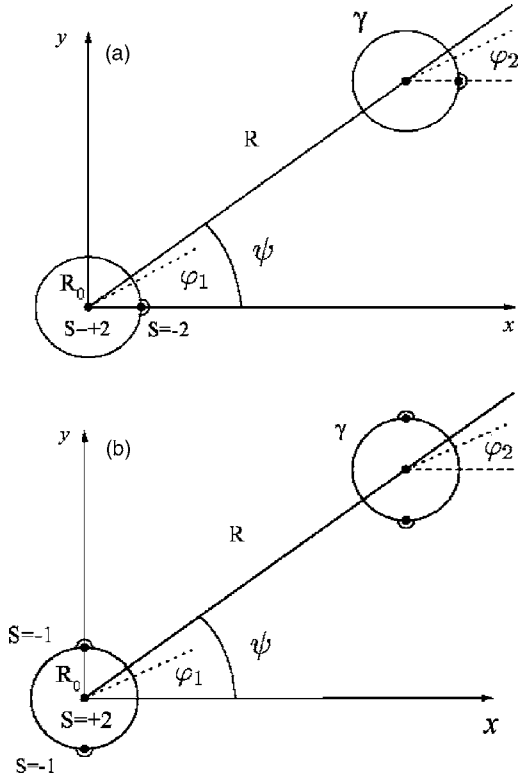


FIG. 4. Schematic representation of inclusions with dipolar (a) and quadrupolar (b) far-field interaction. The distortion formed by the dipolar inclusion (a) is similar to the distortion created by topological defects with $s=+2$ in the center of inclusion and $s=-2$ on its boundary. The distortion formed by the quadrupolar inclusion is equivalent to the field of a topological defect with $s=+2$ in the center of inclusion and two defects with $s=-1$ on its boundary.

solution (3) in polar coordinates may be rewritten in a compact form as

$$\varphi = 3\pi/2 - 2 \arctan \frac{\sin \psi}{(R/R_0) - \cos \psi}. \tag{4}$$

Similarly for the quadrupolar configuration the solution is the superposition of distortions originating from an $s=+2$ defect at the inclusion center and a pair of $-1$ defects located symmetrically around the particle at $y=\pm R_0$ [Fig. 4(b)]:

$$\varphi = 3\pi/2 + 2 \operatorname{Im} \ln(z) - \operatorname{Im} \ln(z - iR_0) - \operatorname{Im} \ln(z + iR_0) \tag{5}$$

or

$$\varphi = 3\pi/2 + \arctan \frac{\sin 2\psi}{(R/R_0)^2 + \cos 2\psi}. \tag{6}$$

Note that the director fields described by Eqs. (4) and (6) are only valid out of the islands. As for the director fields inside the islands, they will be discussed at the end of this section. The long-range parts of these distortions may be obtained from the multipolar expansion of Eq. (4):

$$\varphi = 3\pi/2 - 2\sum_k (R_0/R)^k \sin k\psi/k \tag{7}$$

and Eq. (6)

$$\varphi = 3\pi/2 - \sum_k (-1)^k (R_0/R)^{2k} \sin 2k\psi/k. \tag{8}$$

Expansions start ($k=1$) with dipolar (7) and quadrupolar (8) terms. $P=2R_0$ may be considered as the magnitude of the dipole moment [12] for a droplet-defect pair (two charges $s=+2$ and $-2$ in the dipole). The distance at which essential deformation of the molecular orientation takes place decreases from Coulombic to dipolar and then to quadrupolar configuration. In the latter case the molecular orientations $\varphi=\pm\pi/4$ are realized on the surface of inclusion at $\psi=m\pi/4$. At $R\to\infty$ maximal distortion of the **c** director (deviation from $\varphi=3\pi/2$) asymptotically approaches the same directions $\psi=m\pi/4$. At intermediate distances $R_0<R<(2)^{1/4}R_0$ molecular orientations $\varphi=\pm\pi/4$ (and so the brightest areas) are shifted from $\psi=m\pi/4$ to the directions of point defects [Eq. (6); Figs. 1(c) and 3(b)]. This shift will be discussed later in connection with the interaction between inclusions.

In some cases at the same boundary conditions (planar or radial) the director configurations may exist with defects in the host medium or on the particle surface. In a number of these cases the question of global stability of configurations was answered experimentally or (and) theoretically from the energetic point of view. Transition to the surface-defect structure occurs with decreasing strength of surface anchoring [4]. In a 3D nematic the configuration with Saturn ring around the equatorial plane of the particle (quadrupolar configuration) is stable for small droplet size. With increasing droplet size the equatorial ring collapses into an $s=-1$ point defect [2,4,32,34]. By contrast, in a 2D nematic according to the calculation [15] a pair of defects with $s=-1/2$ located symmetrically around the particle is a stable configuration. As for defects on the droplet boundary the question about stability of different configurations may be solved theoretically only by considering the microscopical structure of the interface. Experimentally we observed not only pure dipolar (single defect) and quadrupolar (two defects located on opposite sides of the inclusion) but also different complex configurations with defects located in intermediate positions [Fig. 5(a)]. Such inclusions form a complex director distortion [Fig. 5(b)]. The horizontal symmetry plane is broken and a dipole moment in the vertical direction is induced. If the point defects are situated on the inclusion boundary under an angle $\beta$, the first terms of the multipolar expansion have the form

$$\varphi = 3\pi/2 - 2(R_0/R)\cos(\beta/2)\sin\psi - (R_0/R)^2 \cos\beta \sin 2\psi. \tag{9}$$

Expression (9) for $\beta=0$ corresponds to the first two terms of the dipolar configuration (7) and for $\beta=\pi$ to the first term of the quadrupolar configuration (8). We should note that the contribution of the dipolar component becomes dominating already at $R/R_0>3$ and for the shift of the defects from inclusion poles to angles about 10°.

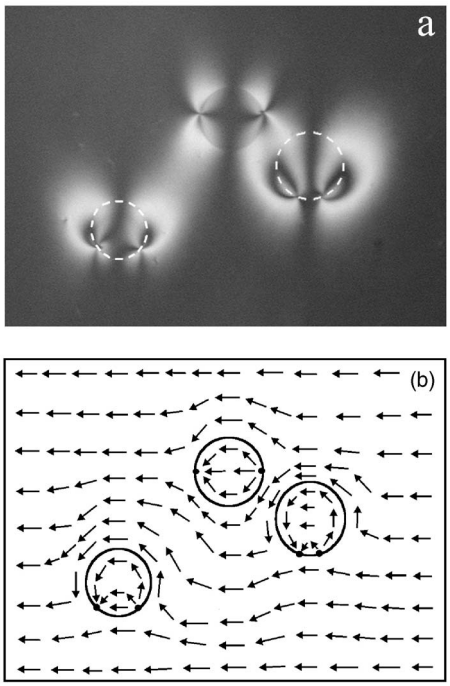


FIG. 5. Smectic islands with crossover from quadrupolar to dipolar **c**-director configurations (a). Dotted lines show the island boundary. The horizontal size of the image is about 540 $\mu$m. UDOBA, $T=127$ °C. Schematic mapping of the **c** director in the membrane (b).

We finish this section with a remark about the physical ("real") and virtual topological defects. The regions outside and inside the inclusions must be considered independently. We start with description of the **c**-director field outside the inclusion. A set of point defects must be introduced [12]. If the companion physical defect localizes at $R=r_d$ outside the inclusion, virtual defects at $R=0$ ($s=+2$) and at $R=R_0^2/r_d$ (one defect with $s=-1$ or two with $s=-1/2$) inside the inclusion would be required [12] to satisfy the boundary conditions and to calculate the director configuration. In our case the positions of surface physical defect(s) and virtual defects with negative topological charges coincide ($r_d=R_0$; Fig. 4). So the defects with $s=+2$ in the center of the droplets (Fig. 4) are virtual defects. There are no physical defects with $s=+2$ in the center of the inclusions (Figs. 3–5).

### B. Director field inside the islands

We will now consider the interior of the inclusion. Since the **c** director inside the island is parallel to the boundary, topology requires the presence of physical defect(s) inside the island. These physical defects have positive topological charges. Texture within the island with one physical topological defect was described by Langer and Sethna [38]. The orientation of the **c**-director field inside the island in Fig. 3(a) is similar to the **c**-director field created by an $s=+2$ defect [38]. In reality only a surface defect with the winding number $s=+1$ exists on the interior side of the island boundary. The orientation of the **c**-director field inside the island in Fig. 3(b) is similar to the **c**-director field created by two $s=+1$ topological defects located on the island boundary:

$$\varphi = 3\pi/2 + \mathrm{Im}\ \ln(z - iR_0) + \mathrm{Im}\ \ln(z + iR_0) \tag{10}$$

or

$$\varphi = 3\pi/2 + \arctan \frac{\sin 2\psi}{(R_0/R)^2 + \cos 2\psi}. \tag{11}$$

In reality two surface defects with winding number (charge) $s=+1/2$ exist on the interior side of the island boundary [Figs. 3(b) and 5]. Planar anchoring on the island boundary and defects induce a nontrivial director configuration within the islands which is shown by arrows in Figs. 3 and 5. In Fig. 3(a) the orientation of the **c** director is constant along any line passing through the defect. Note that the $s=+1$ defect may escape from the boundary inside the island and even transform into a small nematic droplet. Contrary to this, the topology of the **c**-director field requires the location of two $s=+1/2$ boojum defects at the island border [Figs. 3(b) and 5(b)].

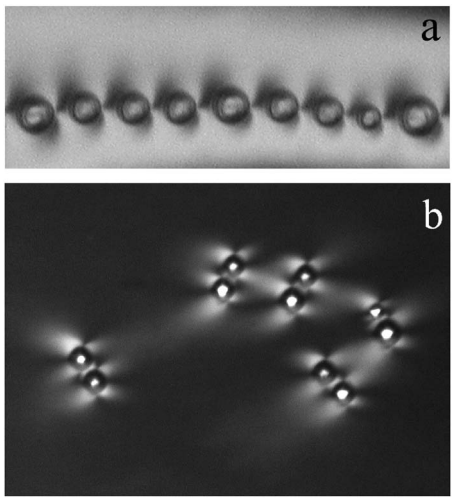


FIG. 6. Oriented chains formed by droplets in smectic membranes with dipolar (a) and quadrupolar (b) interparticle interaction. Pairs of droplets in (b) orient in two symmetric directions with respect to the vertical axis. The **c** director far from the inclusions is oriented along the vertical axis. The picture (b) was observed with the analyzer and polarizer crossed; image (a) with a slightly decrossed analyzer. The horizontal size of the images is about 540 $\mu$m. 50% DOBA, 50% UDOBA, $T=127.1$ °C.

## IV. INTERACTION AND CHAINING OF INCLUSIONS

Overlapping of elastic distortion from two inclusions leads to their interaction, which is anisotropic and may be attractive or repulsive depending on the respective positions of the inclusions. At low concentration the inclusions may form stable chains. For the dipolar configuration a typical droplet chain is shown in Fig. 6(a). Dipolar chains orient perpendicular to the **c** director. This orientation differs drastically from that observed earlier for the case of radial boundary conditions [16,17] when chains oriented parallel to the **c** director. Open squares in Fig. 7 show the interparticle

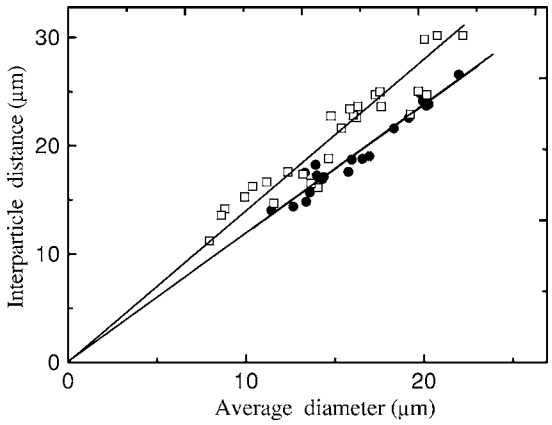


FIG. 7. Interparticle distances $L$ versus average diameter $D_0$ for the droplets in chains with dipolar (open squares) and quadrupolar (closed circles) interactions. Lines correspond to interparticle distance $L=1.4D_0$ (dipoles) and $L=1.2D_0$ (quadrupoles).

distance $L$ (measured between the centers of neighboring particles) as a function of the average diameter $D_0$ of two neighboring inclusions in dipolar chains. The solid line corresponds to interparticle distance $L=1.4D_0$. For the quadrupolar configuration chain formation is similar to that previously observed [19]. In oriented membranes chains may orient in two directions symmetric with respect to the far-field **c** director [Fig. 6(b)] which is parallel to the vertical axis. The angle between the chains and the **c** director at infinity is about 30° and the average interparticle distance $L\approx 1.2D_0$ is smaller than for the dipolar configuration. Our values of $L$ are close to the values of interparticle distance (about $1.3D_0$) for the case when the topological defect is situated in the host medium between the droplets [16] or for droplets with a pair of surface defects [22].

Adapting the results for quadrupolar distortion in a 2D nematic [14] to our case, the long-range two-body interaction may be written for smectic membranes in the multipolar (dipolar or quadrupolar) approximation. The host director field fixes the orientation of droplets. The director distortion $\varphi_{12}$ for large interparticle distance may be presented approximately as a superposition of $\varphi_1$ and $\varphi_2$ solutions for isolated inclusions, $\varphi_{12}\approx\varphi_1+\varphi_2$ [14]. The interaction energy $F_{int}=K/2[\int(\nabla\varphi_{12})^2d^2r-\int(\nabla\varphi_1)^2d^2r-\int(\nabla\varphi_2)^2d^2r]$ in this approximation for identical inclusions is [14]

$$F_{int}\approx K\int \nabla\varphi_1\,\nabla\,\varphi_2 d^2r = 2K\int_\gamma \varphi_2\partial\varphi_1/\partial\mathbf{n}\,d\mathbf{l}, \qquad (12)$$

where $K$ is the elastic Frank constant. The integral is taken over the circular contour $\gamma$ around the second inclusion (Fig. 4) with boundary condition $\varphi_2$, $d\boldsymbol{l}$ is a contour element, and **n** normal to the contour $[\partial\theta/\partial\mathbf{n}=(-\partial\theta/\partial y,\partial\theta/\partial x)]$. Using $\varphi_1$ from Eqs. (7) and (8) and considering the lowest-order terms, integration gives

$$F^d_{int}\approx -8\pi K(R_0/R)^2\cos 2\psi \qquad (13)$$

for dipoles and

$$F^q_{int}\approx 12\pi K(R_0/R)^4\cos 4\psi \qquad (14)$$

for quadrupoles.

Interactions fall off as $R^{-2}$ and $R^{-4}$, respectively, for the dipolar (13) and quadrupolar (14) symmetry ($R^{-3}$ and $R^{-5}$ in 3D systems). For the dipolar configuration the attraction between inclusions at large distances is within the angular sector $(-\pi/4,\pi/4)$. The preferred respective orientation of inclusions (13) is perpendicular to the **c** director which corresponds to minimal distortion (4). This axis is a plane (line in 2D) of symmetry for modulus **c** and for the interaction energy $F_{int}=K/2\int(\nabla\varphi_{12})^2d^2r$ (but not for the **c** vector) and we may expect, as observed in experiment, that chains at short interparticle distances will be also aligned perpendicular to the **c** director. This is the middle direction in the angular sector of attraction $(-\pi/4,\pi/4)$.

For the quadrupolar configuration the favorable orientation of inclusions at large distance (14) is at angles $m\pi/4$ ($m$ is odd) in 2D geometry (~49° with respect to the symmetry axis in 3D [3,33]) which correspond to the maximum distortion (6). However, these lines are not the symmetry directions for our inclusion-defect geometry, so it is difficult to judge about the orientation of the chains at short distances. Numerical calculations for a 2D nematic with defects in the host medium predict a change of the chain orientation with decreasing distance from oblique ($\pi/4$) to the direction coinciding with orientation of defects in an isolated inclusion [14]. The equilibrium configuration is achieved at interparticle distance $L\approx 1.2D_0$ with chain orientation perpendicular to the **n** director [14]. Taking into account the difference in anchoring conditions (radial in [14] and planar in our case) we may guess that the chain orientation in a 2D smectic should be parallel to the **c** director. However, a strong change of orientation at decreasing distance obtained in the theory [14] is accompanied by a shift of the position of defects situated in the host medium. In smectic membranes the defects localize on the inclusion boundary and their shift along the boundary is hampered. Nevertheless, the chain orientation does not correspond to the long-range quadrupolar approximation (14) and the preferred chain orientation is indeed closer to the orientation of the **c** director on large distances. Attraction at large distances is within angular sectors $(\pi/8+k\pi/2,\ 3\pi/8+k\pi/2)$, where $k$ is an integer (14). The chain orientation (about ±30° with respect to the **c** director at infinity) is within these angular sectors of attraction. It is worth noting that at large distances the energy minimum is achieved in the direction of strongest director distortion ($\psi=\pi/4$), just as for close interparticle distances the chain orientation is shifted toward the droplet poles where the distortion is also maximal [bright areas in Figs. 1(c) and 3(b)].

## V. CHAINLIKE SUPERSTRUCTURES AND CLUSTERS

Simple chaining is characteristic for dipolar interaction, for which there are no free bonds inside the chain. For inclusions with quadrupolar distortion two of four bonds [bright regions in Figs. 1(c) and 3(b)] are free if the inclusion is situated in the middle of the chain, and three for the terminal

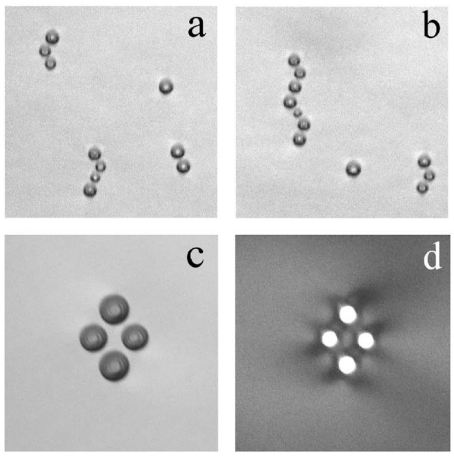


FIG. 8. Clusters formed by droplets with quadrupolar interaction. The **c** director far from the inclusions is oriented along the vertical axis. The nonlinear symmetrical chain (b) and the long diagonal of the rhombi (c), (d)) orient parallel to the **c** director. (a), (b), and (c) were obtained in unpolarized light. In (d) the polarizers are crossed. The horizontal size of the images is about 220 $\mu$m (a), (b) and 150 $\mu$m (c), (d). 25% DOBA, 75% UDOBA, $T=125.6$ °C.

inclusion in the chain. So quadrupolar interaction leads to formation of open structures in which the particles may attach to free bonds. The simplest nonlinear chains and clusters are shown in Fig. 8. The size of the droplets is from 10 to 15 $\mu$m Figs. 8(a) and 8(b) and about 17–21 $\mu$m Figs. 8(c) and 8(d). The structure of nonlinear chains and clusters qualitatively correlates with the two-particle interaction analyzed in Sec. IV. Quadrupolar inclusions may attach to each other in two equivalent directions (+) and (−) with respect to the **c** director at infinity, namely, at angles +30° and −30° (Sec. IV). Nonlinear chains [Figs. 8(a) and 8(b)] form if the inclusions attach to different free bonds (+) and (−). Orientation of the average axis of a nonlinear chain depends on the number and length of its linear parts. If they are arranged symmetrically [Fig. 8(b)], chains orient parallel to the **c** director. Rhombi in Figs. 8(c) and 8(d) are also formed when inclusions attach to (+) and (−) free bonds. The longer diagonal of the four-particle rhombi orients along the **c** director [Figs. 8(c) and 8(d)]. This orientation corresponds to the minimum of elastic energy when the line between topological defects in the inclusion is parallel to the far-field **c** director (Secs. III and IV). The average angle between the neighboring linear parts in nonlinear chains $\alpha_{12}$ is about 50°. In a simple model with two-particle interaction one would expect $\alpha_{12}=\alpha_0$ where $\alpha_0=60°$ is the angle between two different orientations of independent chains (Sec. IV). The difference between $\alpha_{12}$ and $\alpha_0$ indicates the necessity for evoking many-particle interactions for a quantitative description of a cluster.

Inclusions with Coulombic configuration ($s=+1$) do not form stable interparticle structures with inclusions possessing quadrupolar configuration (Fig. 9). The main effect is orientation of single quadrupolar inclusions, chains, and clusters by the field formed by the Coulombic inclusion. Streamlines of the field are circular in Fig. 9 as schematically represented in Fig. 2(a). The long diagonal of the rhombus

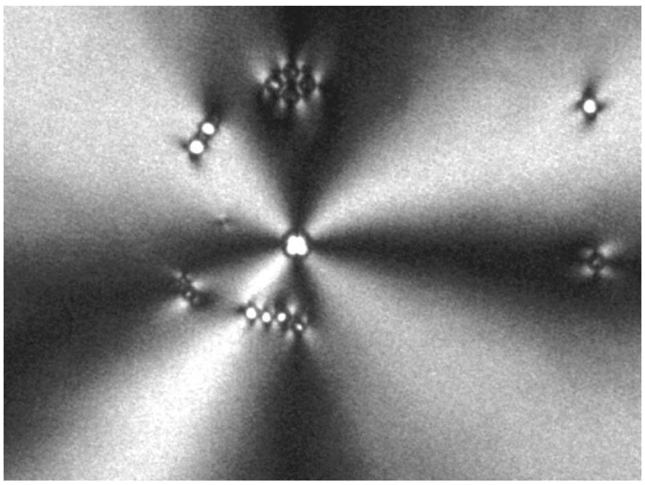

FIG. 9. Orientation of single quadrupolar droplets, chains, and a rhombus in Coulomb director field (circular orientation of the **c** director). They do not form stable structures with a Coulombic particle. The polarizers are crossed. The horizontal size of the image is about 560 $\mu$m. 50% DOBA, 50% UDOBA, $T=125.7$ °C.

and the line connecting the topological defects of the inclusions orient along the streamlines. Effective orientation extends over a long distance from the inclusion with a nonzero topological charge.

Droplets with dipolar interaction in some cases may form branched chains [Fig. 10(a)]. Contrary to quadrupoles with well-defined angles in nonlinear chains, the angle between linear parts of dipolar chains is not fixed and may vary from 60° to about 160°. The central droplet, as well as the other

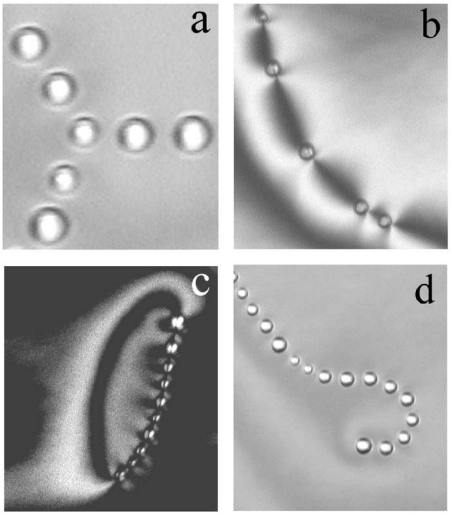


FIG. 10. In membranes with a nonoriented **c** director the dipolar droplets may form branched chains (a). Droplets nucleate preferably in elastically deformed parts of the membrane (b). Orientation of the chain with an accompanying wall (c) does not correspond to the orientation of a single chain (perpendicular to the **c** director). Chains formed by dipolar inclusions could be bent (d). The pictures (a) and (d) were taken in unpolarized light. Images (b) and (c) were made with crossed polarizers. The horizontal size of the images is about 65 $\mu$m (a) and 190 $\mu$m (b), (c), (d). 25% DOBA, 75% UDOBA; $T=127.1$ °C (a), (b), (d), and $T=126.2$ °C (c).

droplets in the branched chain, has only one topological defect which points toward one of the chains. In this chain, the dipoles (dipolar vectors) of droplets are directed toward the central droplet; in two other chains the dipoles are directed away from the central droplet. Branched chains form if two droplets approach the chain simultaneously. More often such branched chains may be observed in membranes with a nonoriented **c**-director field. Droplet nucleation, chain formation, and orientation of both droplets and chains differ essentially in oriented and nonoriented samples. In defect-free membranes the nucleating droplets are positioned randomly [Fig. 1(c)]. In liquid crystal samples with point or line defects droplets nucleate preferably in the regions with a large director gradient [22,26,39,40]. In membranes with $\pi$ walls droplets tend to nucleate inside the walls [Fig. 10(b)]. Such droplets are localized in the center of the wall and moving along it they form a chain. If the ends of the wall are not fixed on the boundary of the membrane, a closed structure is formed. An example of such a structure is shown in Fig. 10(c). Due to the anisotropy of the two-dimensional orientational elasticity ($K_s > K_b$ [28] where $K_s$ and $K_b$ are, respectively, the splay and bend elastic constants) the energy of a $\pi$ wall is minimal when it is oriented parallel to the **c** director. Competition between the preferred orientation of the chain (perpendicular to the **c** director, Sec. IV) and the $\pi$ wall (parallel to the **c** director [28]) leads to an intermediate orientation of the chain accompanied by the wall. This orientation differs essentially from the orientation of chains in the membrane with oriented director field (Sec. IV). We should note that the orientational rigidity of dipolar chains is less than that of the quadrupolar ones, and they may bend [Fig. 10(d)], adjusting to the orientation of the host **c**-director field. Moreover, the interparticle distance in such chains may be larger than in linear ones. However, chains do not dissociate, since they minimize the elastic energy in the region of the deformation of the **c** director [Fig. 10(b)].

## VI. CONCLUSION

Most theoretical studies of arrangement and aggregation of particles in liquid crystals dealt with 3D nematic media with strong or weak director anchoring on the particle surface. Experimentally in 3D media strong anchoring and linear structures were mainly investigated except for the hexagonal arrangement near the surface [6]. In 2D smectic membranes different types of defect localization and inclusion self-organization, most of which have not been described theoretically, were found. The morphology of structures depends on the interparticle interaction. We report on experimental investigation of membranes in which the 2D director field was oriented. Up to now experiments were performed in membranes with nonoriented director field, although theoretical studies implied orientationally ordered samples. We demonstrate that nucleation of inclusions and their self-organization differ sufficiently in membranes with orientationally ordered and unordered **c**-director fields. In nonoriented membranes the formation of structures from inclusions may be determined mainly by the membrane texture [Fig. 10(b)]. Orientation of chains with a line defect [Fig. 10(c)] is essentially changed with respect to the defect-free membrane. Both interparticle distances [Fig. 10(d)] and structures formed by inclusions [e.g., the "star" in Fig. 10(a)] differ in oriented and nonoriented membranes. Formation of clusters and their structure and orientation in disordered membranes (Fig. 10) often cannot be described even qualitatively by existing theory. This indicates once more that for comparison of theory with experiment, oriented membranes must be employed.

We observed inclusions with Coulombic, dipolar, and quadrupolar configurations of 2D director field. Droplets with one (dipole) or two (quadrupole) defects on the droplet boundary form chains oriented perpendicular to the **c** director or at angle about 30° to **c** Formation of chains and clusters in oriented membranes may be understood qualitatively on the base of long-range interparticle interaction and symmetry of the system. Nevertheless the structure of the clusters and chains, their orientations cannot be completely described by two-particle interactions. For a quantitative description of collective inclusion behavior and spatial organization of inclusions, theory has to be developed for 2D systems with localization of topological defects on the inclusion boundary.

## ACKNOWLEDGMENTS

This work was supported by the Russian Foundation for Basic Research Grant No. 05-02-16675, and by Grant No. MK-4057.2005.2.

[1] P. Poulin, H. Stark, T. C. Lubensky, and D. A. Weitz, Science **275**, 1770 (1997).
[2] T. C. Lubensky, D. Pettey, N. Currier, and H. Stark, Phys. Rev. E **57**, 610 (1998).
[3] P. Poulin and D. A. Weitz, Phys. Rev. E **57**, 626 (1998).
[4] H. Stark, Eur. Phys. J. B **10**, 311 (1999).
[5] J.-C. Loudet, P. Barois, and P. Poulin, Nature (London) **407**, 611 (2000).
[6] V. G. Nazarenko, A. B. Nych, and B. I. Lev, Phys. Rev. Lett. **87**, 075504 (2001).
[7] W. Russel, D. Saville, and W. Schowalter, *Colloidal Dispersions* (Cambridge University Press, Cambridge, U.K., 1989).
[8] C. Lapointe, A. Hultgren, D. M. Silevitch, E. J. Felton, D. H. Reich, and R. L. Leheny, Science **303**, 652 (2004).
[9] W. H. de Jeu, B. I. Ostrovskii, and A. N. Shalaginov, Rev. Mod. Phys. **75**, 181 (2003).
[10] C. Y. Young, R. Pindak, N. A. Clark, and R. B. Meyer, Phys. Rev. Lett. **40**, 773 (1978).
[11] P. G. de Gennes and J. Prost, *The Physics of Liquid Crystals*, 2nd ed. (Clarendon Press, Oxford, 1993).
[12] D. Pettey, T. C. Lubensky, and D. Link, Liq. Cryst. **25**, 597 (1998).

[13] J. I. Fukuda, B. I. Lev, and H. Yokoyama, Phys. Rev. E **65**, 031710 (2002).
[14] M. Tasinkevych, N. M. Silvestre, P. Patrício, and M. M. Telo da Gama, Eur. Phys. J. E **9**, 341 (2002).
[15] J. Fukuda and H. Yokoyama, Eur. Phys. J. E **4**, 389 (2001).
[16] P. Cluzeau, P. Poulin, G. Joly, and H. T. Nguyen, Phys. Rev. E **63**, 031702 (2001).
[17] P. Cluzeau, V. Dolganov, P. Poulin, G. Joly, and H. T. Nguyen, Mol. Cryst. Liq. Cryst. Sci. Technol., Sect. A **364**, 381 (2001).
[18] P. Cluzeau, G. Joly, H. T. Nguyen, and V. K. Dolganov, Pis'ma Zh. Eksp. Teor. Fiz. **75**, 573 (2002) [JETP Lett. **75**, 573 (2002)].
[19] P. Cluzeau, G. Joly, H. T. Nguyen, and V. K. Dolganov, Pis'ma Zh. Eksp. Teor. Fiz. **76**, 411 (2002) [JETP Lett. **76**, 351 (2002)].
[20] P. V. Dolganov, E. I. Demikhov, B. M. Bolotin, V. K. Dolganov, and K. Krohn, Eur. Phys. J. E **12**, 593 (2003).
[21] P. Cluzeau, F. Bougrioua, G. Joly, L. Lejček, and H. T. Nguyen, Liq. Cryst. **31**, 719 (2004).
[22] C. Völtz and R. Stannarius, Phys. Rev. E **70**, 061702 (2004).
[23] D. Demus, *Flüssige Kristalle, in Tabllen* (VEB Deutscher fur Grundstoff Industrie, Leipzig, 1974).
[24] M. Born and E. Wolf, *Principles of Optics* (Pergamon, Oxford, 1980).
[25] T. Stoebe, P. Mach, and C. C. Huang, Phys. Rev. Lett. **73**, 1384 (1994).
[26] P. Cluzeau, G. Joly, H. T. Nguyen, C. Gors, and V. K. Dolganov, Liq. Cryst. **29**, 505 (2002).
[27] P. V. Dolganov, P. Cluzeau, G. Joly, V. K. Dolganov, and H. T. Nguyen, Phys. Rev. E **72**, 031713 (2005).
[28] P. V. Dolganov and B. M. Bolotin, Pis'ma Zh. Eksp. Teor. Fiz. **77**, 503 (2003) [JETP Lett. **77**, 429 (2003)].
[29] B. I. Lev, S. B. Chernyshuk, P. M. Tomchuk, and H. Yokoyama, Phys. Rev. E **65**, 021709 (2002).
[30] F. Picano, R. Hołyst, and P. Oswald, Phys. Rev. E **62**, 3747 (2000).
[31] Y. Hatwalne and T. C. Lubensky, Phys. Rev. E **52**, 6240 (1995).
[32] E. M. Terentjev, Phys. Rev. E **51**, 1330 (1995).
[33] S. Ramaswamy, R. Nityananda, V. A. Raghunathan, and J. Prost, Mol. Cryst. Liq. Cryst. Sci. Technol., Sect. A **288**, 175 (1996).
[34] P. Poulin, V. Cabuil, and D. A. Weitz, Phys. Rev. Lett. **79**, 4862 (1997).
[35] R. W. Ruhwandl and E. M. Terentjev, Phys. Rev. E **55**, 2958 (1997).
[36] O. Mondoin-Monval, J. C. Dedien, T. Gulik-Krzywicki, and P. Poulin, Eur. Phys. J. B **12**, 167 (1999).
[37] A. N. Chuvyrov, A. P. Krekhov, Yu. A. Lebedev, N. Kh. Gil'manova, Zh. Eksp. Teor. Fiz. **89**, 2052 (1985); [Sov. Phys. JETP **62**, 1183 (1985)].
[38] S. A. Langer and J. P. Sethna, Phys. Rev. A **34**, 5035 (1986).
[39] H. Schüring and R. Stannarius, Langmuir **18**, 9735 (2002).
[40] C. Völtz and R. Stannarius, Phys. Rev. E **72**, 011705 (2005).